

The Effect of Pinning on Drag in Coupled One-Dimensional Channels of Particles

C. BAIRNSFATHER, C.J. OLSON REICHHARDT AND C. REICHHARDT

Theoretical Division, Los Alamos National Laboratory, Los Alamos, New Mexico 87545
Department of Physics, Purdue University, West Lafayette, Indiana 47907

PACS 82.70.Dd – Colloids
 PACS 05.60.Cd – Classical transport

Abstract. - We consider a simple model for examining the effects of quenched disorder on drag consisting of particles interacting via a Yukawa potential that are placed in two coupled one-dimensional channels. The particles in one channel are driven and experience a drag from the undriven particles in the second channel. In the absence of pinning, for a finite driving force there is no pinned phase; instead, there are two dynamical regimes of completely coupled or locked flow and partially coupled flow. When pinning is added to one or both channels, we find that a remarkably rich variety of dynamical phases and drag effects arise that can be clearly identified by features in the velocity force curves. The presence of quenched disorder in only the undriven channel can induce a pinned phase in both channels. Above the depinning transition, the drag on the driven particles decreases with increasing pinning strength, and for high enough pinning strength, the particles in the undriven channel reach a reentrant pinned phase which produces a complete decoupling of the channels. We map out the dynamic phase diagrams as a function of pinning strength and the density of pinning in each channel. Our results may be relevant for understanding drag coupling in 1D Wigner crystal phases, and the effects we observe could also be explored using colloids in coupled channels produced with optical arrays, vortices in nanostructured superconductors, or other layered systems where drag effects arise.

There are many examples of one- and two-dimensional (1D and 2D) coupled bilayers or coupled channels of interacting particles, including vortices in superconducting bilayers [1, 2], colloidal systems [3–6], dusty plasmas [7], and Wigner crystals [8–10]. In many of these systems it is possible to apply an external drive to one of the layers and measure the resulting response of the other layer as well as the drag effect produced by the particles in the undriven layer on those in the driven layer. For instance, this type of measurement has been performed for the transformer geometry in two-layer superconducting vortex systems [1, 2]. If the vortices in each layer are completely coupled, the measured response is the same in both layers. If instead the vortices are only partially coupled between layers, the response is reduced in the undriven layer compared to the driven layer. A similar coupling-decoupling transition is also predicted for coupled wires containing 1D Wigner crystals [8], and certain drag effects in 1D wires have been interpreted as resulting from the formation of 1D Wigner crystal states [9].

Many of these systems can contain some form of quenched disorder which could produce pinning effects [11]; however, very little is known about how pinning alters the drag or transport properties in layered geometries. The quenched disorder could be strong in one channel and weak in another, or it could be of equal strength in both channels, resulting in different types of dynamic phases. Particles driven over random quenched disorder in single layer systems are known to exhibit a variety of dynamical phases associated with distinct transport signatures, as shown in simulations [11–14] and experiments [15]. These studies suggest that distinct dynamics could also arise in a two-layer drag system when pinning is present. We note that there have been studies of two-layer driven colloidal systems; however, the effect of quenched disorder was not considered [4].

In this work we propose a simple model of two coupled 1D channels of particles with repulsive Yukawa interactions where there a drive channel and a drag channel, and where pinning is added to one or both channels. Despite

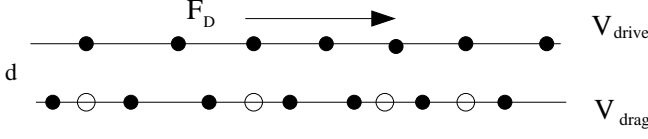


Fig. 1: A schematic of the system of two coupled 1D channels separated by a distance d . Each channel contains N particles (black dots) which interact via a Yukawa potential with particles in the same and the adjacent channel. An external drive F_D is applied to the particles in the drive channel, resulting in an average particle velocity of V_{drive} in the drive channel. The velocity response in the drag channel is V_{drag} . Quenched disorder is introduced in the form of localized pinning sites (open circles) of maximum force F_p which are spaced randomly in the channel without overlapping. The pinning can be placed only in the drag channel (as shown), only in the drive channel, or in both channels.

the apparent simplicity of this system, we find that a remarkably rich variety of distinct dynamical phases are possible which produce pronounced changes in the transport and drag effects. Although our model treats 1D channels, we expect that many of the same effects should be generic to coupled layer systems with quenched disorder. The specific system we consider could be realized experimentally using colloidal particles in channel geometries [16] where a driving force is applied to one channel via optical means or an electric field. The effects we observe could also be studied with coupled 1D Wigner crystals [9, 11, 17, 18] or in superconductors with nanofabricated channel geometries [19] when the current is applied to only one channel and the response is measured in both channels. In our system, we find that without pinning there is a finite drive transition from a locked regime to a partially decoupled regime in which the response of the drag channel decreases with increasing drive. Addition of pinning to the drag channel can induce a pinned phase for both channels. As the drive increases, both channels depin into a locked or partially locked phase, followed at high drives by a reentrant pinning of the drag channel when the dynamic coupling of the two channels becomes weak enough. When the driving force is fixed at a low value, increasing the strength of the pinning in the drag channel increases the effective drag on the particles in the driven channel; for higher fixed driving force, however, increasing the pinning strength reduces the drag on the driven channel and causes the channels to decouple when the drag channel becomes reentrantly pinned. We also observe strong fluctuations in both channels at the locked to partially locked transition for intermediate strengths of quenched disorder. We map out the evolution of the dynamical phases for a wide variety of parameters including pinning in both channels, pinning in only one of the channels, and for varied pinning densities.

Simulation- In fig. 1 we show a schematic of our system which consists of two 1D channels separated by a distance d with periodic boundary conditions in the x -direction. Each channel contains N particles which interact via a re-

pulsive Yukawa potential with other particles in the same channel and with particles in adjacent channels. Particles in the upper or drive channel are subjected to an applied external force F_D . A single particle i located at position \mathbf{R}_i undergoes motion obtained by integrating the overdamped equation of motion:

$$\eta \frac{d\mathbf{R}_i}{dt} = \mathbf{F}_i^{pp} + \mathbf{F}_i^s + \mathbf{F}_i^D. \quad (1)$$

Here η is the damping constant which is set to $\eta = 1.0$. The particle-particle interaction force is $\mathbf{F}_i^{pp} = \sum_{j \neq i}^{2N} -\nabla V(R_{ij})$ where $V(R_{ij}) = (E_0/R_{ij}) \exp(-\kappa R_{ij}) \hat{\mathbf{R}}_{ij}$, $R_{ij} = |\mathbf{R}_i - \mathbf{R}_j|$, $\hat{\mathbf{R}}_{ij} = (\mathbf{R}_i - \mathbf{R}_j)/R_{ij}$, and $E_0 = Z^{*2}/4\pi\epsilon\epsilon_0 a_0$. Here ϵ is the solvent dielectric constant, Z^* is the effective charge, and $1/\kappa$ is the screening length. In each channel, the average particle spacing is a and we take $d/a = 2/3$. We also take $1/\kappa = 2d$ to ensure that coupling between the two channels is possible. We note that we have also considered other values of d , a , and κ and find the same qualitative features, indicating that our results should be generic for this class of system. The pinning force \mathbf{F}_i^s arises from N_p attractive parabolic potentials with a maximum force of F_p and a radius of $R_p = 0.5$, $\mathbf{F}_i^p = \sum_{k=1}^{N_p} E_0 F_p (R_{ik}^p/R_p) \Theta(R_p - R_{ik}) \hat{\mathbf{R}}_{ik}^p$. Here Θ is the Heaviside step function, \mathbf{R}_k^p is the location of pinning site k , $R_{ik}^p = |\mathbf{R}_i - \mathbf{R}_k^p|$, and $\hat{\mathbf{R}}_{ik}^p = (\mathbf{R}_i - \mathbf{R}_k^p)/R_{ik}^p$. In this work we consider the limit in which the number of pinning sites is smaller than or similar to the number of particles in the system; however, we find the same qualitative features when we change the pinning density or strength. The external force F_D is applied only to the particles in the driven channel. We increase F_D from zero in small increments of $\delta F_D = 0.001$, spending a waiting time of 10^4 simulation time steps at each increment. We measure the average velocity of the particles in the drive and drag channels, $V_{drag} = N_{drag}^{-1} \sum_{i=1}^{N_{drag}} d\mathbf{x}_i/dt$ and $V_{drive} = N_{drive}^{-1} \sum_{i=1}^{N_{drive}} d\mathbf{x}_i/dt$, where $N_{drag} = N$ is the number of particles in the drag channel and $N_{drive} = N$ is the number of particles in the drive channel. This simulation method, employing overdamped dynamics with random pinning, has been used previously to explore the behavior of colloids driven over random and periodic substrates as well as two layer systems. A similar method has been used to study sliding Wigner crystals and vortices in type-II superconductors.

In fig. 2(a) we show the velocity force curves V_{drive} and V_{drag} versus F_D for the case where there is no pinning in either channel. At low F_D , $V_{drive} = V_{drag}$, indicating that the particles are moving together in the coupled region (C). At $F_D = 2.0$, the average particle velocity in each channel is just under 1.0. In the absence of the drag channel, we would have $V_{drive} = 2.0$ at $F_D = 2.0$ since $V = F_D/\eta$ under our overdamped dynamics. When the drive channel is locked with the drag channel, the same driving force must be used to transport twice as

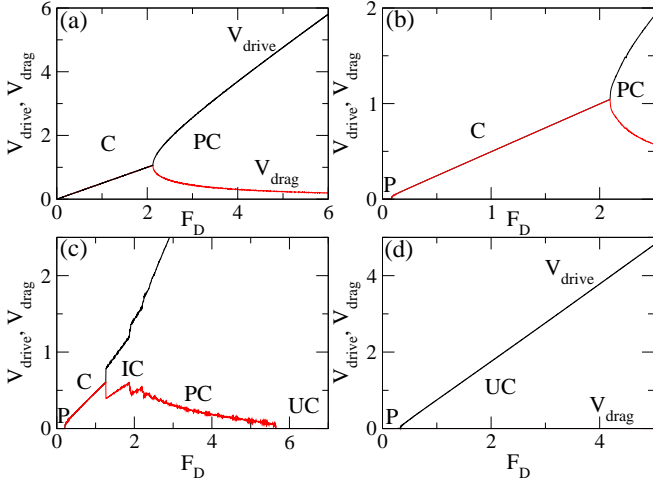


Fig. 2: The average particle velocity in the drive channel V_{drive} and the drag channel V_{drag} vs applied force F_D for a sample with pinning in the drag channel at $N_p/N = 0.083$. (a) The pin-free case $F_p = 0.0$ has two regions: an initial coupled region (C) where motion in both channels is completely locked, and a partially coupled (PC) region where V_{drag} monotonically decreases while V_{drive} increases with increasing F_D . (b) For $F_p = 1.0$ there is an initial pinned region (P) in both channels in addition to the C and PC regions. (c) At $F_p = 2.5$, an intermittent region (IC) containing a series of asymmetric jumps in V_{drag} appears between the C and the PC regions. At $F_D = 5.66$ there is a reentrant pinning of the drag channel above which $V_{drag} = 0.0$, producing an uncoupled region (UC). (d) At $F_p = 4.0$, only the P and UC regions appear and $V_{drag} = 0$ for all F_D .

many particles, reducing the particle velocity by half. At $F_D = 2.124$ there is a transition to a partially coupled (PC) state where the velocity curves branch apart. V_{drive} continues to increase with increasing F_D with a slope higher than the slope of V_{drive} below $F_D = 2.124$, while V_{drag} decreases with increasing F_D . Since there is no pinning, in the PC region V_{drag} gets smaller and smaller with increasing F_D but never reaches zero. The general shape of the velocity force curves is very similar to the response observed for the superconducting transformer geometry where vortices in a pair of adjacent superconducting layers can couple and decouple depending on the applied current [1, 2]. In the superconducting system, the voltage response is proportional to the particle velocity and the applied current is proportional to F_D . Additionally, the velocity-force curves in fig. 2(a) are in agreement with the predicted coupling-decoupling transition for disorder-free coupled 1D Wigner crystal systems [8].

In fig. 2(b) we plot V_{drive} and V_{drag} versus F_D for a system containing pinning in the drag channel with $N_p/N = 0.083$ and $F_p = 1.0$. The curves are similar to the pin free case, but a pinned region (P) now appears for $F_D < 0.1$ when the quenched disorder in the drag channel causes the particles in both channels to stop moving. The particles in the drag channel are directly pinned by the

pinning sites, but the particles in the driven channel are only indirectly pinned by their interactions with the particles in the drag channel, which produce an effective periodic pinning potential for the driven particles. The driven particles can either simply move over this periodic potential, in which case we find a decoupled region (UC) where the driven particles are moving and the drag particles are pinned, or the driven particles can drag the periodic potential along with them, depinning the drag particles and producing a moving coupled region. As F_D increases, there is a transition from the coupled to partially coupled flow at the same $F_D = 2.124$ as in the pin-free system. Figure 2(c) shows the velocity-force curves for a sample with $F_p = 2.5$, where the transition out of region C falls at a lower $F_D = 1.26$ and is followed by a region containing a series of jumps in both V_{drive} and V_{drag} . In this intermittently coupled (IC) region, each downward jump in V_{drag} is preceded by a range of F_D over which V_{drag} increases linearly with increasing F_D . The jumps in V_{drag} are accompanied by similar sharp upward jumps in the value of V_{drive} . As F_D increases, the jumps decrease in size until the system crosses over to the partially coupled (PC) region where V_{drag} decreases linearly and smoothly with increasing F_D . At high F_D , the uncoupled channel (UC) region appears when the particles in the drag channel become pinned again for $F_D \geq 5.66$ but the particles in the driven channel continue to flow. The reentrant pinning of the drag channels results when the effective dynamical coupling between the two channels weakens for higher F_D , as indicated by the decrease in V_{drag} with increasing F_D in the PC region of the pin-free sample shown in fig. 2(a). When the dynamical coupling between the channels drops below a critical value, the drag force experienced by the particles in the drag channel falls below the depinning threshold for the pinning sites in the drag channel, resulting in the repinning transition. We expect this reentrant pinning effect to be a generic feature in drag systems containing quenched disorder, and its signature is a sudden decrease of the drag channel response to zero. In fig. 2(d) for $F_p = 4.0$, the drag channel never depins over the range of F_D shown, and there is a single transition from region P where both channels are pinned to the decoupled region UC.

In fig. 3(a) we plot the dynamic phase diagram F_D versus F_p for the system in fig. 2 containing pinning only in the drag channel. The transition between the PC and UC regions drops to lower values of F_D with increasing F_p since a lower drive is required to reduce the effective drag force below the depinning threshold of the drag channel at higher F_p . For $F_p > 3.88$, only the P and UC regions appear. The extent of region C decreases with increasing F_p until region C disappears for $F_p > 3.45$. The IC region vanishes at higher values of F_D and reaches its maximum extent near $F_p = 2.95$. In fig. 3(b) we plot V_{drive} versus F_p for the same system at fixed $F_D = 0.2$. Here V_{drive} decreases with increasing F_p until the system enters the pinned region at $F_p = 2.0$ and V_{drive} drops to zero. The

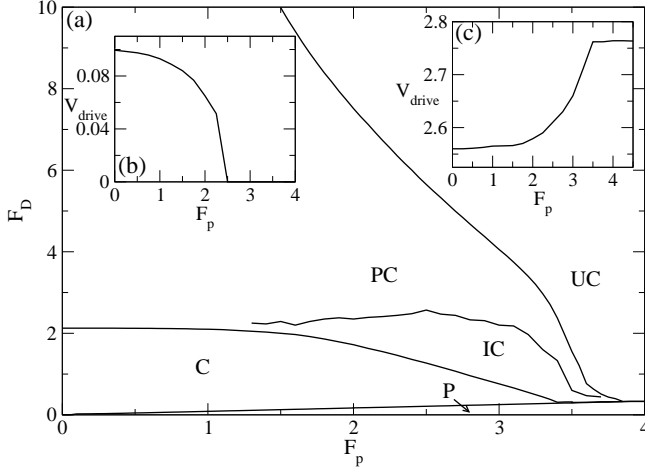


Fig. 3: (a) The dynamic phase diagram of F_D vs F_p for the system in fig. 2 for pinning in only the drag channel. Each region is marked: pinned (P), coupled (C), intermittently coupled (IC), partially coupled (PC), and uncoupled (UC). (b) V_{drive} versus F_p from the system in (a) at $F_D = 0.2$. The increasing effective damping $\eta^* = F_D/V_{drive}$ produces a monotonic decrease in V_{drive} with increasing F_p until the particles in the driven channel repin and the velocity drops to zero in region P . (c) V_{drive} vs F_D for the system in (a) at $F_D = 3.0$. Here V_{drive} increases with increasing F_p until the onset of the UC phase, above which V_{drive} saturates to a constant value.

effective damping of the driven particles, $\eta^* = F_D/V_{drive}$, increases with increasing F_p . In fig. 3(c) we show V_{drive} versus F_p at fixed $F_D = 3.0$, where V_{drive} monotonically increases until the system enters the UC phase, and V_{drive} saturates to a constant value. These results show that pinning in the drag channel can either increase or decrease the effective drag on the driven channel depending on the strength of the pinning and the amplitude of the dc drive.

We next consider a system containing pinning in both channels. Figure 4(a) shows the dynamic phase diagram of F_D versus F_p for a sample with a pinning density of $N_p/N = 0.083$ in each channel. The overall shape of the phase diagram resembles the phase diagram in fig. 3(a) obtained with pinning in only the drag channel. The pinned phase P grows in size with increasing F_p much more rapidly when there is pinning in both channels than when there is pinning in only the drag channel. In fig. 4(c) we plot V_{drive} and V_{drag} versus F_D at $F_p = 4.0$ for the sample from fig. 4(a) with pinning in both channels. When V_{drag} drops to zero at $F_D = 2.22$ at the transition to region UC , there is a jump up in the value of V_{drive} . In fig. 4(b) we show the phase diagram of F_D versus F_p for a sample containing pinning in only the drive channel with $N_p/N = 1.33$. The UC phase no longer appears since the particles in the drag channel can only reentrantly repin when there is pinning in the drag channel. For $F_p > 5.5$, the system crosses directly from region P to region PC without passing through the C region. Figure 4(d) illustrates V_{drive} and V_{drag} versus F_D for this system at

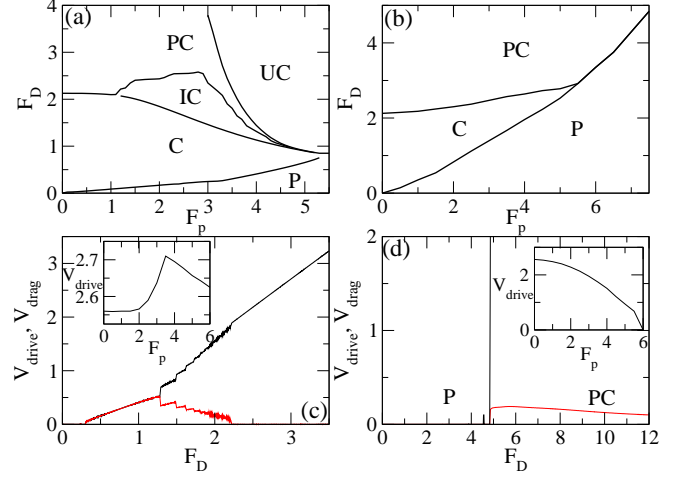


Fig. 4: (a) The dynamic phase diagram of F_D vs F_p for a system with pinning in both channels. Each channel has $N_p/N = 0.083$. The region labels are the same as in fig. 3(a). (b) The dynamic phase diagram of F_D vs F_p for a system with pinning in only the drive channel, with $N_p/N = 1.33$. Here the uncoupled channel region is absent and there can be a direct transition from region P to region PC . (c) V_{drive} (upper curve) and V_{drag} (lower curve) vs F_D for the system in (a) at $F_p = 4.0$. Inset: V_{drive} vs F_p for the system in (a) at $F_D = 3.0$. (d) V_{drive} (upper curve) and V_{drag} (lower curve) vs F_D for the system in (b) at $F_p = 7.5$. Inset: V_{drive} vs F_p for the system in (b) at $F_D = 3.0$.

$F_p = 7.5$. There is a transition directly from region P to region PC at $F_D = 4.8$, and above this drive V_{drag} gradually decreases with increasing F_D .

In the inset of fig. 4(c) we plot V_{drive} versus F_p at $F_D = 3.0$ for the system in fig. 4(a) where there is pinning in both channels. For $F_p < 3.5$, V_{drag} increases with increasing F_p , just as shown in fig. 3(c) for the sample with pinning in only the drag channel. For $F_p > 3.5$, when there is pinning in both channels V_{drag} decreases with increasing F_p for $F_p > 3.5$ rather than saturating. The increase in V_{drag} with increasing F_p for $F_p < 3.5$ results when the pinning in the drag channel reduces the coupling between the driven and drag particles. For $F_p > 3.5$ at $F_D = 3.0$, the particles in the drag channel are always pinned. If there is pinning in only the drag channel, V_{drive} remains constant for $F_p > 3.5$ as shown in fig. 3(c); however, if pinning is also present in the drive channel, it produces an increasing drag on the driven particles, causing V_{drive} to decrease with increasing F_p at $F_p > 3.5$ for the sample with pinning in both channels. In the inset of fig. 4(d) we illustrate this effect more clearly by plotting V_{drive} vs F_p for a system with pinning in only the drive channel. Here V_{drive} monotonically decreases with increasing F_p until it reaches zero once all the drive particles become pinned.

It is also possible to vary d/a , where d is the distance between the channels and a is the average particle spacing within the channels. We consider the effect of varying particle density in samples with fixed d . Increasing the

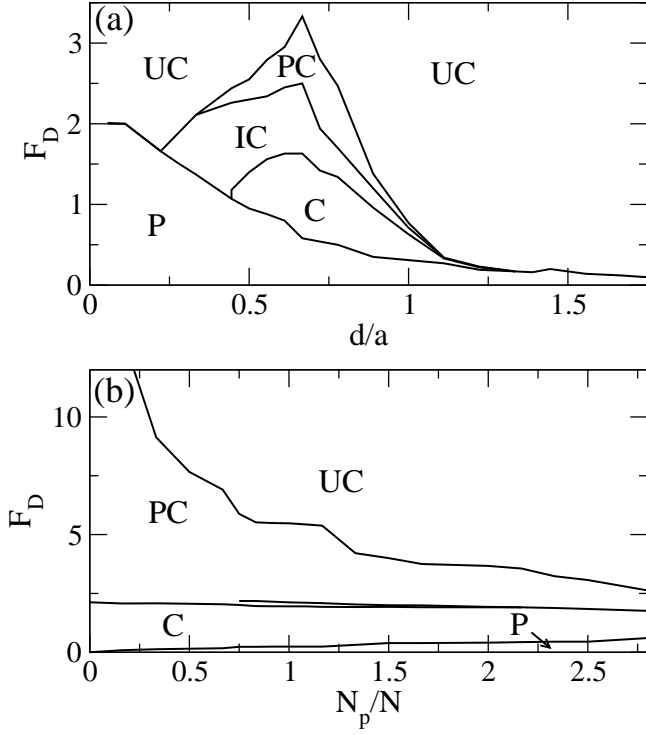


Fig. 5: (a) The dynamic phase diagram of F_D vs d/a for a sample with pinning in both channels at $F_p = 2.0$ and with $N_p/N = 0.25$ at $d/a = 0.67$. (b) The dynamic phase diagram of F_D vs N_p/N for a sample with pinning in both channels at $d/a = 0.67$ and $F_p = 1.0$.

particle density reduces the effective coupling between the channels since the periodic potential experienced by the particles in one channel produced by the particles in the other channel becomes smoother as the particle density increases. In fig. 5(a) we plot the dynamic phase diagram for F_D versus d/a in a sample with pinning in both channels for fixed $F_p = 2.0$ and with $N_p/N = 0.25$ at $d/a = 0.67$. At low d/a , there is a large pinned region since the particles within each channel are far from each other, strongly enhancing the effectiveness of an individual pinning site. For $d/a < 0.22$, the system passes directly from region P to region UC . For large d/a , each particle interacts strongly with other particles in the same channel but the coupling to particles in the other channel is greatly reduced, so the system again crosses directly from the pinned to the UC region. For intermediate values of d/a , the three other regions C , IC , and PC appear in windows between the P and UC regions. The total width of these intermediate windows reaches a peak at $d/a = 0.66$. In fig. 5(b) we show the dynamic phase diagram of F_D versus the pinning density N_p/N for a system with pinning in only the drag channel at $F_p = 1.0$ and $d/a = 0.67$. The transition from region PC to region UC drops to lower F_D with increasing N_p/N since higher pinning density causes the repinning threshold in the drag channel to decrease.

The transition between region C and region PC also shifts to lower F_D with increasing N_p/N , and there is a narrow window (not labeled on the figure) where region IC appears between regions C and PC . There is also a small plateau in all of the transitions near $N_p/N = 1.0$, which is a weak commensuration effect. For periodically arranged pinning sites, we expect much stronger commensuration effects to occur; these effects will be considered elsewhere.

In summary, we introduce a simple model to study the effects of pinning on drag in coupled one-dimensional channels of particles interacting via a Yukawa potential where a drive is applied to only one channel. This system exhibits a rich variety of dynamical phases which are associated with distinct features in the velocity-force curves. In the absence of pinning, at low drives both channels are coupled and exhibit identical particle velocities. As the drive is increased, there is a transition to a partially coupled phase where the velocity in the drag channel decreases with increasing drive while the velocity in the driven channel increases with increasing drive. Placing pinning in only the drag channel produces a region in which both channels are pinned as well as a reentrant pinning of the particles in the drag channel at higher drives when the coupling between the channels is dynamically weakened. When strong pinning is placed either in the drag channel or in both channels, we observe only a pinned region and a decoupled region. For intermediate pinning strength, we find a strongly fluctuating region where a series of asymmetric jumps appear in the velocity-force curves. Increasing the strength of the pinning in the drag channel generally reduces the effective drag on the particles in the driven channel at higher drives since the pinned particles in the drag channel are unable to absorb momentum from the particles in the drive channel. We map the dynamic phase diagrams for samples with pinning in both channels, pinning in only the drive channel, and pinning in only the drag channel. The smallest number of phases appears for pinning in only the drive channel, while samples with pinning in both channels exhibit multiple dynamical phase transitions even when the particle density or pinning density is altered, showing that the effects we observe are robust for a wide range of parameters. Our results could be important for understanding drag effects in systems where 1D Wigner crystal states can occur and for understanding the general effects of quenched disorder in other drag and transformer geometries. Additionally, our system could be directly realized experimentally for colloidal or dusty plasma systems in coupled 1D channels. Extensions of this model that could be explored include the effects of a periodic pinning array at and away from commensurability, as well as the effects of disorder on the coupling of particles confined in adjacent two-dimensional planes.

This work was carried out under the auspices of the NNSA of the U.S. DoE at LANL under Contract No. DE-

AC52-06NA25396.

REFERENCES

- [1] GIAEVER I., *Phys. Rev. Lett.*, **15** (1965) 825.
- [2] CLEM J.R., *Phys. Rev. B*, **9** (1974) 898; EKin J.W., SERIN B. and CLEM J.R., *Phys. Rev. B*, **9** (1974) 912.
- [3] MESSINA R. and LÖWEN H., *Phys. Rev. Lett.*, **91** (2006) 146101.
- [4] DAS M., ANANTHAKRISHNA G. and RAMASWAMY S., *Phys. Rev. E*, **68** (2003) 061402; MESSINA R. and LÖWEN H., *Phys. Rev. E*, **73** (2006) 011405.
- [5] LUTZ C., KOLLMANN M. and BECHINGER C., *Phys. Rev. Lett.*, **93** (2004) 026001;
- [6] HERRERA-VELARDE S., ZAMUDIO-OJEDA A. and CASTAÑEDA-PRIEGO R., *J. Chem. Phys.*, **133** (2010) 114902; COSTE C., DELFAU J.-B., EVEN C. and SAINT JEAN M., *Phys. Rev. E*, **81** (2010) 051201.
- [7] HARTMANN P., DONKÓ Z., KALMAN G.J., KYRKOS S., GOLDEN K.I. and ROSENBERG M., *Phys. Rev. Lett.*, **103** (2009) 245002.
- [8] BAKER J. and ROJO A.G., *J. Phys.: Condens. Matter*, **13** (2001) 5313.
- [9] YAMAMOTO M., STOPA M., TOKURA Y., HIRAYAMA Y. and TARUCHA S., *Science*, **313** (2006) 204.
- [10] GOLDONI G. and PEETERS F.M., *Phys. Rev. B*, **53** (1996) 4591.
- [11] PIACENTE G. and PEETERS F.M., *Phys. Rev. B*, **72** (2005) 205208.
- [12] KOSHELEV A.E. and VINOKUR V.M., *Phys. Rev. Lett.*, **73** (1994) 3580; FALESKI M.C., MARCHETTI M.C. and MIDDLETON A.A., *Phys. Rev. B*, **54** (1996) 12427; OLSON C.J., REICHHARDT C. and NORI F., *Phys. Rev. Lett.*, **81** (1998) 3757; KOLTON A.B., DOMÍNGUEZ D. and GRØNBECH-JENSEN N., *Phys. Rev. Lett.*, **83** (1999) 3061; Fily Y., OLIVE E., DI SCALA N. and SORÉ J.C., *Phys. Rev. B*, **82** (2010) 134519.
- [13] REICHHARDT C. and OLSON C.J., *Phys. Rev. Lett.*, **89** (2002) 078301; CHEN J.X., CAO Y. and JIAO Z., *Phys. Rev. E*, **69** (2004) 041403; REICHHARDT C. and OLSON C.J., *Phys. Rev. E*, **79** (2009) 061403; SENGUPTA A., SENGUPTA S. and MENON G.I., *Phys. Rev. B*, **81** (2010) 144521.
- [14] REICHHARDT C. and OLSON C.J., *Phys. Rev. Lett.*, **93** (2004) 176405.
- [15] BHATTACHARYA S. and HIGGINS M.J., *Phys. Rev. Lett.*, **70** (1993) 2617; PARDO F., DE LA CRUZ F., GAMMEL P.L., BUCHER E. and BISHOP D.J., *Nature*, **396** (1998) 348; PERTSINIDIS A. and LING X.S., *Phys. Rev. Lett.*, **100** (2008) 028303; GUITERREZ J., SILHANEK A.V., VAN DE VONDEL J., GILLIJNS W. and MOSHCHALOV V.V., *Phys. Rev. B*, **80** (2009) 140514(R); AVCI S., XIAO Z.L., HUA J., IMRE A., DIVAN R., PEARSON J., WELP U., KWOK W.K. and CRABTREE G.W., *Appl. Phys. Lett.*, **97** (2010) 042511.
- [16] KÖPPL M., HENSELER P., ERBE A., NIELABA P. and LEIDERER P., *Phys. Rev. Lett.*, **97** (2006) 208302; BLEIL S., REIMANN P. and BECHINGER C., *Phys. Rev. E*, **75** (2007) 031117.
- [17] PIACENTE G., SCHWEIGERT I.V., BETOURAS J.J. and PEETERS F.M., *Phys. Rev. B*, **69** (2004) 045324; PIACENTE G., HAI G.Q. and PEETERS F.M., *Phys. Rev. B*, **81** (2010) 024108.
- [18] DESHPANDE V.V. and BOCKRATH M., *Nature Phys.*, **4** (2008) 314.
- [19] BESSELING R., KES P.H., DRÖSE T. and VINOKUR V.M., *New J. Phys.*, **7** (2005) 71; YU K., HEITMANN T.W., SONG C., DEFEO M.P., PLOURDE B.L.T., HESSELBERTH M.B.S. and KES P.H., *Phys. Rev. B*, **76** (2007) 220507(R).